frontiers | Frontiers in Marine Science

TYPE Original Research
PUBLISHED 12 June 2024
DOI 10.3389/fmars.2024.1305674

OPEN ACCESS

EDITED BY
Thanos Dailianis,
Hellenic Centre for Marine Research (HCMR), Greece

REVIEWED BY
Wyatt Million,
University of Technology Sydney, Australia
Natalia Carabantes,
CICESE, Mexico

*CORRESPONDENCE
Silvia Arossa
silvia.arossa@kaust.edu.sa

RECEIVED 02 October 2023
ACCEPTED 27 May 2024
PUBLISHED 12 June 2024

CITATION
Arossa S, Klein SG, Garuglieri E, Steckbauer A, Parry AJ, Alva Garcia JV, Alamoudi T, Yang X, Hung S-H, Salazar OR, Marasco R, Fusi M, Aranda M, Daffonchio D and Duarte CM (2024) Oxygen supersaturation adds resistance to a cnidarian: Symbiodiniaceae holobiont under moderate warming in experimental settings.
Front. Mar. Sci. 11:1305674.
doi: 10.3389/fmars.2024.1305674

Oxygen supersaturation adds resistance to a cnidarian: Symbiodiniaceae holobiont under moderate warming in experimental settings

Silvia Arossa[1,2,3]*, Shannon G. Klein[1,2,3], Elisa Garuglieri[2], Alexandra Steckbauer[1,2,3], Anieka J. Parry[1,2,3], Jacqueline V. Alva Garcia[1,2,3], Taiba Alamoudi[1,2,3], Xinyuan Yang[2], Shiou-Han Hung[1,2], Octavio R. Salazar[1,2], Ramona Marasco[2], Marco Fusi[4,5], Manuel Aranda[1,2], Daniele Daffonchio[2] and Carlos M. Duarte[1,2,3]

[1]Marine Science Program, Biological and Environmental Science and Engineering Division, King Abdullah University of Science and Technology (KAUST), Thuwal, Saudi Arabia, [2]Red Sea Research Center (RSRC), King Abdullah University of Science and Technology, King Abdullah University of Science and Technology (KAUST), Thuwal, Saudi Arabia, [3]Computational Bioscience Research Center (CBRC), King Abdullah University of Science and Technology, King Abdullah University of Science and Technology (KAUST), Thuwal, Saudi Arabia, [4]Joint Nature Conservation Committee, Peterborough, United Kingdom, [5]Centre for Conservation and Restoration Science, Edinburgh Napier University, Edinburgh, United Kingdom

Ocean warming reduces O_2 solubility and increases organismal O_2 demand, endangering marine life. Coastal ecosystems, however, experience O_2 supersaturation during peak daytime temperatures due to metabolic cycles. Recent discoveries show that this environmental supersaturation can reduce the vulnerability of tropical species to warming by satisfying their oxygen requirements. To test whether this also occurs within the cnidarian holobiont, we elevated internal O_2 in *Cassiopea andromeda* at nighttime (i.e. holobiont respiration prevails on Symbiodniaceae O_2 production) relying on bell pulsation for ventilation, then experimentally subjected them to thermal stress (+1°C day^{-1}). Though ecologically unrealistic, this approach verified our hypothesis and eliminated confounding factors. Holobionts were exposed to either constant levels of 100% air saturation (100AS) or nighttime supersaturation (NSS; where 100% air saturation transitioned to O_2 supersaturation at nighttime). At sublethal temperatures, supersaturation mitigated reductions in holobiont size of ~ 10.37% (-33.418% $\pm$ 0.345 under 100AS vs -23.039% $\pm$ 0.687 under NSS). Supersaturation alleviated chlorophyll-*a* loss by 42.73% until 34°C, when counteraction of this process could not be sustained due to excessive thermal stress. Supersaturation also enriched potentially beneficial bacterial taxa of the microbiome and selected a more consistent bacterial community. Although modest, the detected effects show that a O_2 surplus increased the resistance of the holobionts to thermal stress.

KEYWORDS

oxygen supersaturation, cnidarian, endosymbiosis, ocean warming, cnidarian microbiome

Introduction

Ocean warming drives oxygen loss (deoxygenation) in both open ocean and coastal ecosystems (Klein et al., 2020). Particularly, rising temperatures widen oxygen depleted areas (Stramma et al., 2008; Hughes et al., 2020) and constrain oxygen (O_2) availability *via* reduced solubility (Vaquer-Sunyer and Duarte, 2011) and heightened respiratory demand of marine organisms (Pörtner and Farrell, 2008; Vaquer-Sunyer and Duarte, 2011; Klein et al., 2020). Hence, a mechanistic understanding of how marine biota respond to temperature-induced changes in dissolved O_2 is vital, especially in the tropics where climate-driven alterations of the tropical thermocline already restrict O_2 levels (Deutsch et al., 2011; Stramma and Schmidtko, 2021).

Reduced O_2 availability may limit the ability of the marine biota to meet the heightened metabolic demand during heatwave events (Pörtner, 2012). Rising temperatures commonly increase O_2 threshold for hypoxemia (i.e. the below-normal O_2 level in body fluids) in marine organisms (Vaquer-Sunyer and Duarte, 2011; Giomi et al., 2019). O_2 availability in the marine environment thus becomes a major resource determining the survival of biota under thermal stress (Pörtner and Farrell, 2008; Vaquer-Sunyer and Duarte, 2011; Alderdice et al., 2022). This implies that processes that produce O_2, such as photosynthesis, play a particularly important role in supporting the metabolic O_2 demand of marine organisms under thermal stress (Pörtner et al., 2006; Giomi et al., 2019). Also, increased O_2 availability was observed enhancing calcification in calcifying cnidarians (Colombo-Pallotta et al., 2010).

Tropical coastal ecosystems, including mangrove forests, seagrass meadows, and coral reefs, exhibit extreme diel fluctuations in temperature and O_2 (e.g., Giomi et al., 2019, 2023; Pezner et al., 2023). Coastal ecosystems in the Red Sea are extreme examples of this, with fluctuations of O_2 from <2 mg $L^{-1}$to 14 mg L^{-1} (Roik et al., 2016; Giomi et al., 2019, 2023) and temperature from ~29°C to 43°C (Saderne et al., 2019). These trends are coupled through thermodynamic and metabolic processes (Ohde and van Woesik, 1999; Klein et al., 2019; Giomi et al., 2023). Diel O_2 minima characteristically co-occur with lower temperature levels prior to dawn, owing to community respiration (Giomi et al., 2019, 2023). Conversely, during the daytime, when community productivity dominates, O_2 levels can reach extremely high values (defined as O_2 supersaturation, >100% air saturation and even >140%) that coincide with peak daytime temperatures in the mid-afternoon (McArley et al., 2020; Giomi et al., 2019, 2023, respectively). Similar variations occur also in other coastal regions across the tropics (e.g., Ohde and van Woesik, 1999) and temperate regions (Trowbridge et al., 2017). Fluctuations are mainly driven by intense community metabolism, reduced depth, and limited ventilation and/or water exchange, which are characteristic of coastal areas (Klein et al., 2020), and can be intensified by specific local conditions, i.e. metabolic, biogeochemical, and physical processes. Such variations can be moderated by ocean warming (Yu et al., 2015; Chaidez et al., 2017; Klein et al., 2019) and usually exceed diel oscillations reported for the open ocean (Claret et al., 2018; Klein et al., 2019).

These extreme variations in O_2 levels are also experienced internally by the cnidarian holobionts. Indeed, microsensor measurements have revealed that their internal tissues experience extreme light/dark oxygen cycles, ranging from hypoxia to supersaturation (e.g., ~5–710 µmol L-1 in *Acropora* sp.; Kühl et al., 1995; ~ 2–17.5 mg L^{-1} in *Cassiopea* sp.; Arossa et al., 2021), highlighting the potential for significant oxidative stress and the critical role of antioxidant defenses in mitigating its effects. Moreover, the hypothesis that diel O_2 supersaturation, driven by endosymbionts' photosynthetic activity, could alleviate the impacts of thermal stress has yet to be thoroughly explored. Confirming this would not only reveal a previously unrecognized advantage of the cnidarian-Symbiodiniaceae symbiosis but also emphasize the symbiosis's contribution to enhancing holobiont thermal tolerance.

Oxidative stress, resulting from a combination of Symbiodiniaceae photosynthetic activity and environmental stressors, has been implicated as a primary driver of bleaching in cnidarians (Lesser, 2011; Roth, 2014), among other processes (e.g., protein and lipid peroxidation, and DNA damage; Halliwell and Gutteridge, 1999). Oxidative defenses serve as primary protective line against these potential damages (Furla et al., 2011). Despite this, recent studies have cast doubt on the universal applicability of the oxidative stress-driven bleaching hypothesis, finding insufficient evidence in specific cases like *Exaiptasia diaphana* (Dungan et al., 2022), *Pocillopora damicornis* (Nielsen et al., 2018), and in broader field observations (Diaz et al., 2016). Indeed, cnidarians seem to possess highly efficient antioxidant defenses (Furla et al., 2011) and have an intrinsic tolerance to varying O_2 levels (Richier et al., 2003; Warner and Suggett, 2016). To further complicate this picture, the dynamic responses of the cnidarian holobiont do not only depend on the cnidarian host and micro-algal symbionts but also on an intricate community of bacteria, fungi, and viruses, also known as their microbiome (Kwong et al., 2019). Indeed, changes in temperature and O_2 levels affect Cnidaria's bacterial communities (Carabantes et al., 2022), which in turn influence holobiont stress tolerance. For instance, heat-tolerant bacteria enhance host protection through mechanisms like antioxidant compounds and heat-shock proteins production (Berkelmans and Van Oppen, 2006), crucially shaping the holobiont's environmental response (Ainsworth et al., 2010; Hector et al., 2022)."

Here, we test whether O_2 supersaturation improves the performance of a non-calcifying cnidarian holobiont under thermal stress. We do so by using the *Cassiopea andromeda* holobiont, as a convenient model of the cnidarian-Symbiodiniaceae symbiosis. Since this relationship is obligate (Freeman et al., 2016), we opted to not use the comparison between aposymbiotic and symbiotic individuals in this experiment due to the adverse effects of bleaching procedures to obtain aposymbiotic specimens (Carabantes et al., 2022). Hence to exclude symbionts' O_2 production, which would otherwise supersaturate tissues in both experimental groups, we chose to experimentally increase the internal O_2 conditions of the holobiont during nighttime (i.e. when Symbiodiniaceae consumes, rather than produce O_2) *via* manipulation of the seawater medium. This allowed us to mimic daytime internal O_2 levels, mimicking

symbiont oxygen production (see Arossa et al., 2021), relying on the capacity of *C. andromeda* to ventilate their internal tissues (Welsh et al., 2009; Durieux et al., 2023). Although this approach represents the natural inverse of the O_2 within holobiont tissues, manipulating nighttime O_2 levels permitted to test whether an internal O_2 surplus could mitigate the effects of thermal stress. For this, we compared the responses of *C. andromeda* during a thermal stress assay exposed to either constant levels of 100% air saturation (~6 mg L^{-1}), or a diel cycle where daytime levels were set at ~6 mg/L and transitioned to supersaturated conditions (~10 mg L^{-1}) at nighttime. Temperature conditions were increased from 30°C to 38°C at a rate of 1°C per day during an 8-day experiment under a photoperiod of 12:12 hours of light: dark. We measured internal O_2 concentrations using microsensors and measured a suite of holobiont biological responses, including photochemical efficiency, chlorophyll-*a* content, Symbiodiniaceae cell density, and composition, antioxidant defenses, holobiont behavior, and changes in the microbiome.

Materials and methods

Experimental approach

In June 2021, 48 holobionts of the model cnidarian *C. andromeda* (details in Supplementary Methods) were collected in the Ibn Sina Research Station lagoon of the King Abdullah University of Science and Technology (KAUST, Makkah district, Saudi Arabia) on the East coast of the Central Red Sea (Latitude: 22.340905N, Longitude: 39.09024E; 0.20 – 1 m depth). The holobionts were acclimated to laboratory conditions for three days prior to the experiment by maintaining them at 30°C ± 0.01 SE under a 12:12 hours light: dark cycle (1989.0 µmol photons m^{-2} s^{-1} ± 124.0 SE) in 2 L glass aquaria. The aquaria were evenly and randomly distributed among four 300L water baths, which were then used for the actual experiment. Each water bath was equipped with a thermometer, temperature controller, two heaters, and a pump that collectively maintained the desired temperature. During the acclimation phase, the aquaria were constantly bubbled with air, maintaining "100AS" and the holobionts were fed daily with newly hatched *Artemia* nauplii. Water was exchanged each day few hours after feeding.

The experimental design consisted of two O_2 treatments: (i) constant levels of "100AS" (81.43% ± 16.05 SD or 5.72 mg L^{-1} ± 0.64 SD), and (ii) "100AS" during the daytime (i.e. 83.00% ± 5.36 SD or 5.89 mg L^{-1} ± 0.56 SD from 6:00 AM to 6:00 PM) and "supersaturation" during the night (i.e. 132.61% ± 16.05 SD or 9.43 mg L^{-1} ± 0.69 SD from 6:00 PM to 6:00 AM). The experimental treatments were designed to replicate conditions of 100AS, here considered as ~ 6 mg L^{-1}, and daytime oxygen supersaturation scenarios detailed in Arossa et al. (2021). Arossa and colleagues reported daytime oxygen supersaturation levels of ~ 17 mg L^{-1}. However, achieving these levels was not feasible in our study due to constraints associated with our gas delivery system. To achieve the nominal O_2 treatments, four sets of three mass flow controllers (MFCs; Omega®) delivered mixtures of pure oxygen (O_2), nitrogen (N_2), and CO_2 gas to the seawater. Two sets of MFCs and were allocated to each O_2 treatment and controlled via LabVIEW Software (*sensu* Klein et al., 2017). For each treatment, the gases were mixed in stainless-steel manifolds and delivered in equal quantities before entering secondary stainless-steel manifolds that were used to adjust the flow rates manually. Air stones were used to gently diffuse the gas mixtures in the seawater of each replicate aquaria. Automatic transitioning between the two O_2 levels of the second treatment was accomplished over 2 hours via the LabVIEW Software. We refer to these treatments throughout the manuscript as "100% air saturation" (100AS) and "nighttime supersaturation" (NSS), respectively. Temperature conditions were increased from 30°C at a rate of 1°C per day using 300-watt titanium heaters (Schego Teichheizer, Germany) and cooling controllers (D-D The Aquarium Solution Ltd), during an 8-day experiment, under a photoperiod of 12:12 hours of light: dark. The temperature increase (+8°C) aligns with the Red Sea's inherent variability (Saderne et al., 2019), and the rate (+1°C per day), in line with Safaie et al. (2018) and prior research (e.g., Voolstra et al., 2020), was selected. While a temperature control group would have been ideal, logistical constraints due to the experiment's sacrificial nature and limited holobionts availability led to its exclusion, enhancing statistical power for inter-treatment comparisons. These factors also limited the frequency of the measurements of the biological responses: those with no sacrificial nature were taken each day, whereas those with sacrificial nature were performed at specific intervals (see Supplementary Figure 1). Twenty-four *C. andromeda* holobionts were randomly allocated to each O_2 treatment (i.e. N = 48; Supplementary Figure 1). Replicates consisted of one holobiont that was immersed in a 2 L glass aquarium. The replicate aquaria were evenly distributed among four 300L water baths that maintained the desired temperatures. Each water bath was equipped with a thermometer, temperature controller, two heaters, and a pump and contained 12 glass aquaria (six per each treatment, 48 in total, Supplementary Figure 1). A photosynthetically active radiation (PAR) sensor (Odyssey®, Odipar) was used to measure the light conditions in the replicate aquaria throughout the experiment. During the experiment, both feeding of the holobionts with newly hatched *Artemia* nauplii and partial seawater exchange were performed daily (Supplementary Table 1).

Since the *Cassiopea*-Symbiodiniaceae relationship is obligate (Freeman et al., 2016), we opted to not use the comparison between aposymbiotic and symbiotic individuals in this experiment due to the adverse effects of bleaching procedures to obtain aposymbiotic specimens (Carabantes et al., 2022). Hence to exclude symbionts' O_2 production, which would otherwise supersaturate tissues in both experimental groups, we chose to experimentally increase internal O_2 conditions of the holobiont during nighttime (i.e. when Symbiodiniaceae consume, rather than produce O_2). We did so via manipulation of O_2 concentrations in seawater medium, relying on the capacity of *C. andromeda* to ventilate their internal tissues *via* bell pulsation (Welsh et al., 2009; Durieux et al., 2023). This allowed us to mimic daytime internal O_2 levels (see Arossa et al., 2021), mimicking symbiont oxygen production. Both our treatments were however hyperoxic if compared to normal nighttime conditions measured under natural conditions (see Arossa et al., 2021). Though ecologically unrealistic, this approach was used as a mechanistic test to verify our hypothesis that greater oxygen availability would moderate the holobiont's response to warming and removed potential confounding factors, such as

potential side-effects due to the treatment to obtain aposymbiotic specimens. During the experiment, malfunctions in the temperature control system and incidents where individuals became entangled in the bubblers, resulting in injury, led to the removal of 17 holobionts. Consequently, the sample size for each treatment for non-invasive measurements varied across different temperature points: 21 individuals at both 30°C and 31°C, 19 at 32°C, 16 at 33°C, 12 at 34°C and 35°C, 9 at 36°C, and 6 at 38°C. In contrast, the sample size for invasive measurements remained consistent, with n = 3 for each temperature treatment.

Biological responses measured

Holobionts were supplemented daily with freshly hatched *Artemia* at ~ 4.00 AM before the start of all measurements (Supplementary Table 1). Then, for each replicate aquarium, we measured holobiont behavior (i.e. bell pulsations) and photochemical efficiency daily. Bell pulsations were used as an indicator of the overall health status of the holobionts, as it allows food capture, expulsion of waste, release of gametes and, most importantly, gases exchange *via* the generation of water flows (Welsh et al., 2009). Bell pulsation rates (BPR) were measured by visually counting the number of bell contractions that occurred in 1 minute while keeping the aquaria inside the water baths to avoid disturbance. Photochemical efficiency (*Fv/Fm*) was measured after counting the BPR (to avoid potential disturbance on the bell pulsation rate) on four randomly selected oral arms, using a Mini-pulse amplitude modulator (MiniPAM, Waltz GmbH, Germany). Observations were made with a major focus on holobiont orientation, lack of pulsations, and/or mucus production. These are commonly considered signs of stress (Béziat and Kunzmann, 2022). Holobionts were considered dead when not moving, unresponsive to stimulus, and when melting was observed.

On days 0, 4, and 6 of the experiment, three holobionts were then randomly selected (per each treatment, Supplementary Table 1) for internal O_2 measurements, symbiont count, chlorophyll-*a* and protein content. Internal O_2 vertical profiles were performed on one oral arm (where 74.5% of total symbionts are hosted; Verde and McCloskey, 1998), using 50 µm-diameter tip O_2 microsensors (OX-50, Unisense Denmark), following an overnight polarization and calibration at O_2 partial pressures of 0 and 21 kPa as previously described (Brune et al., 1995). Microsensors were connected to a motorized micromanipulator controlled by Unisense software and manually positioned above the oral arm (Arossa et al., 2021). Once the microsensor's tip perforated the tissue, we remotely controlled it to perform measurements every 50 µm. Control profiles were obtained by measuring seawater profiles of O_2 to account for eventual background sources of disturbance.

The oral arms used for microsensor measurements (in their entirety) were cut into smaller sections and stored at -20°C for chlorophyll-*a* content, total protein, ITS2 sequencing, and Symbiodiniaceae density analyses following a protocol adapted from (Klein et al., 2019; details in Supplementary Methods). Marginal appendages and vesicles were included in the analyses. A 200 µL aliquot was subsampled from the initial oral arm homogenate and processed to estimate chlorophyll-*a* content via 100% ethanol overnight extraction and standardized to the total protein content (details in Supplementary Methods).

A 1.5 mL aliquot of the remaining homogenate of the oral arms was transferred into 2 mL sterile tubes, then centrifuged for 10 min at 13000 × g at 4°C. The clear supernatant was then subdivided into three aliquots (each one dedicated to a different enzymatic assay), snap-frozen and stored at -80°C. On the day of the measurement, samples were thawed on ice and used respectively in the Superoxide Dismutase (SOD) Activity Assay Kit (colorimetric, Sigma Aldrich) and the Glutathione-S-Transferase (GST) Assay Kit (colorimetric, Sigma Aldrich). All enzymatic assays were carried out following manufacturers' instructions. Reaction readings were performed with an Infinite 200 pro spectrophotometer (TECAN) in transparent 96-wells transparent plates (Corning). Results were calculated following manufacturers' indications and normalized on protein content.

The bell diameter was measured at full extension using a ruler to the nearest mm and percent change in bell size was calculated (see Supplementary Methods for details) only on the jellyfish that lasted until the end of the experiment. At this step, photos of the specimens were taken to evaluate potential bleaching and discoloration. Temperature and gas mixtures were changed at 6 AM. Therefore, each day, all the biological measurements and samples were taken before the temperature change (e.g., on day 0, they were taken at 30°C, on day 1, at 31°C, etc.).

DNA extraction, ITS2 sequencing and Symbiodiniaceae identification

One mL of the homogenate used for the previous analyses was used for Illumina sequencing of the Internal Transcriber Space 2 (ITS2) region to characterize the symbionts community inside *C. andromeda* oral arms (modified from Herrera et al., 2020; details in Supplementary Methods). The sequencing reads obtained with this method were used to identify the Symbiodiniaceae populations using the online database SymPortal (SymPortal; Hume et al., 2019). Briefly, ITS2 sequencing data were used to identify Symbiodiniaceae populations within the *C. andromeda* used in this study. MiSeq ITS2 sequencing reads were analysed using the SymPortal analytical framework (Hume et al., 2019), which uses ITS2 profiles to resolve and classify Symbiodiniaceae diversity. The SymPortal analytical framework pipeline was used to resolve Symbiodiniaceae populations within the *C. andromeda* (Klein et al., 2019). Raw sequence of ITS2 sequencing data have been deposited in the Sequence Read Archives with NCBI BioProject accession no. PRJNA966908.

Total DNA extraction for microbiome analyses

The oral arms not used for the previous analyses were entirely (including mesoglea, gastroderma, colored vescicles, and mucus)

and immediately snap-frozen and stored at –80°C until processed. Then, they were thawed on ice and homogenised entirely (Schuett and Doepke, 2010) in ceramic mortars under sterile conditions. Homogenates were transferred in 1.5 mL sterile tubes, snap-frozen, and stored at –80°C. On the extraction day, samples were thawed on ice and extracted following an adapted version of the protocol described by Robbins and colleagues (Robbins et al., 2021; details in Supplementary Methods). The same protocol was used to extract DNA from three oral arms from three untreated holobionts as "natural microbiome". These specimens were collected from the field on the same day and location as the others. Oral arms were cut after collection, snap-frozen, and stored at –80°C until processed. Similarly, seawater (5 L) was collected from the field in the same site (i.e. environmental microbiome) and was filtered through 0.2 µm sterile polyethersulfone (PES) Sterivex filters (Millipore) using a peristaltic pump (Millipore). Filters were stored at –20°C until DNA extraction. The total DNA was extracted following a modified version of the Phenol-Chloroform protocol described by Michoud and colleagues (Michoud et al., 2021) using lysis buffer, lysozyme solution, and SDS-PK solution described above for holobionts tissues. The same protocol of filtration and extraction was performed on three samples of 30 mL high-density *Artemia salina* culture collected from the same batch administered to the animals as food.

DNA quantification was performed using a Qubit 3.0 Fluorometer with the Qubit dsDNA BR assay kit (Thermo-Fisher Scientific), and quality assessments were carried out by both electrophoresis on 0.8% agarose gels and Nanodrop Drop One Spectrophotometer (Thermo-Fisher Scientific). Extracted DNA was stored at –20°C.

Amplification of the bacterial 16S rRNA gene, metabarcoding library preparation and sequencing

The hypervariable V3–V4 regions of the bacterial 16S rRNA gene were amplified by nested PCR (details in Supplementary Methods). In these reactions the primers synthesised with the appropriate overhang adapter sequences for the Illumina MiSeq system. Both PCR reactions were performed with the addition of 0.5 µM each of universal pPNA and mPNA clamps to reduce the amplification of host and dietary chloroplasts and mitochondria (Fitzpatrick et al., 2018). A blank of DNA extraction and PCR reagents were also amplified with the same protocol and used in the further steps of indexing and sequencing as negative controls. All the amplicon products were used to incorporate the sequencing adapters using the 96 Nextera XT Index Kit (Illumina). The PCR products were further pooled together, concentrated in a CentriVap DNA Concentrator (Labconco) and sequenced with the Illumina MiSeq platform (V3, 300 bp paired-end) at the Bioscience Core Lab, King Abdullah University of Science and Technology (Saudi Arabia). Raw sequence data have been deposited in the Sequence Read Archives with NCBI BioProject accession no. PRJNA964583.

Seawater chemistry characterization

Seawater carbonate chemistry was characterized according to Supplementary Table 1. Briefly, pH and dissolved oxygen were characterized multiple times at specific intervals, while Total Alkalinity (TA) was measured at the beginning, mid, and end of the experiment (i.e. day 0, 4, and 6) every 6 hours to capture potential changes over diel cycles (see Supplementary Table 1).Fifty mL aliquots were taken from three randomly selected aquaria, poisoned with 10 µL of $HgCl_2$ (stock solution of 7 g of $HgCl_2$ in 100 mL water) to prevent biological activity, and then analysed within 2–3 months of sampling. TA was quantified by open-cell titration with 0.1 M hydrochloric acid using the Alkalinity Titrator (MODEL AS-ALK2, Apollo SciTech) with two pumps (VersaPump6, KLOHN) and a pH meter (Orion Star A2II, ThermoFisher) using a pH sensor (SI Analytics). pH was measured using a pH electrode (Mettler Toledo) on the NBS scale (pH_{NBS}). Additionally, temperature and salinity measurements were taken using a temperature sensor and a refractometer, respectively. See Supplementary Methods for determination of seawater carbonate system parameters and detailed calibration protocols.

Data analysis

Environmental and biological data

After testing data for normality, Linear Mixed Models (LMMs) were used to analyse the dependent variables of size percent change, bell pulsation rate, photochemical efficiency, chlorophyll, symbiont density, glutathione-S-transferase, and superoxide dismutase using IBM® SPSS® Statistics software (Version 27.0.1.0). *Post hoc* analyses with multiple pairwise comparisons were performed using the same software as necessary to test differences among the means of our data. Details can be found in Supplementary Methods.

Microbiome amplicon sequence data

Analyses of amplicon sequences were performed using the standard QIIME2, pipeline v2021.2 (Bolyen et al., 2019); details are reported in Supplementary Methods. The compositional similarity matrix (Bray-Curtis, BC) of the log-transformed OUTs table calculations, principal component analysis (PCoA), and multivariate generalised linear models (GLMs) were performed as described in Supplementary Methods. The overall distances from the centroid in 100AS and NSS were analysed by *t*-test as described in Supplementary Methods. The FAPROTAX database assigned bacterial OTUs to known metabolic or ecological functions (http://www.zoology.ubc.ca/louca/FAPROTAX; Louca et al., 2016); 40% of the OTUs were assigned to at least one functional group, while the remaining 60% could not be assigned to any group (leftovers).

Canonical analysis of the principal coordinate was used to compute and explore the difference in predicted functions between O_2 treatment and temperatures in Primer 6 (Anderson and Walsh, 2013). Tax4Fun2 R package (Wemheuer et al., 2020) was further used to compute the predicted functional redundancy of the bacterial community of the holobionts oral arms.

Results

Environmental conditions and internal O_2 levels

Temperature was ramped at a rate of 1°C day^{-1}, according to the experimental design in both "NSS" and "100AS" (Supplementary Figure 2). At night, dO_2 was equal to 132.61 ± 16.05 1SD % air saturation (9.43 ± 0.69 mg L^{-1}) and 78.85 ± 8.18 1SD % air saturation (5.57 ± 0.55 mg L^{-1}) in the "NSS" and "100AS" treatments, respectively (Supplementary Figures 3A, B). During the day, average dO_2 was equal to 83.00 ± 5.36 1SD % air saturation (5.89 ± 0.55 mg L^{-1}) and 84.01 ± 11.02 1SD % air saturation (5.88 ± 0.72 mg L^{-1}) in the "NSS" and "100AS" treatments, respectively (Supplementary Figures 3A, B).

Overall average internal levels of dO_2 reached ~7.48 ± 0.65 1SD mg L^{-1} in the "NSS" treatment and were ~5.67 ± 0.57 1SD mg L^{-1} in the "100AS" treatment ($p < 0.001$, $df = 1$, Denominator $df = 46.770$, F = 17.316, LMMs, AR[1], Figure 1). A decrease in dO_2 was observed with depth in the tentacle ($p < 0.001$, $df = 40$, Denominator $df = 317.755$, F = 4.198, LMMs, AR[1]), whereas temperature effect was not significant ($p = 0.148$, $df = 2$, Denominator $df = 46.770$, F = 1.993, LMMs, AR(1)). The pH was kept stable over the duration of the experiment (Supplementary Figure 3), while TA (µmol Kg^{-1}) and carbon dioxide partial pressure (pCO_2, µatm) showed higher variability towards the end of the experiment (Supplementary Figures 5, 6, respectively).

Biological responses of the holobiont and Symbiodiniaceae characterization

Size percent change (PC, %; Figure 2A) differed between O_2 levels, but this response depended on the temperature, resulting in a significant Oxygen × Temperature interaction (Supplementary Table 2). Specifically, PC followed a decreasing trend, and was significantly higher in the "NSS" treatment than under "100AS" at 36°C (8.40% higher) and non-significantly higher at 37°C, while the opposite was observed at 35°C (non-significant). The overall decrease in size was -23.039% ± 0.687% in the "NSS" treatment, compared to -33.418% ± 0.345% under "100AS". Therefore, holobiont fitness, here defined as size, was overall better maintained under "NSS" conditions (by about 10.37%) at 36°C, while at 37°C the decrease in size was not significantly different between the two O_2 levels due to high variability. However, differences between the two O_2 levels were inconsistent throughout the experiment (Supplementary Tables 3, 4). Melting and heavy mucus release was first observed at 36°C under "100AS" (Supplementary Videos 1, 2).

The increasing temperature caused a rise in bell pulsation rate (BPR; Figure 2B; Supplementary Tables 5, 6) and a decrease in photochemical efficiency (*Fv/Fm*) (Figure 2C; Supplementary Table 6), but no effects mediated by O_2 treatments were observed (Supplementary Tables 5, 6). Significant differences in BPR among temperatures were observed throughout the experiment, but mainly between low (e.g., 30°C) and high temperatures (e.g., 36–37°C). Photochemical efficiency significantly differed among almost all the temperatures (Supplementary Table 6).

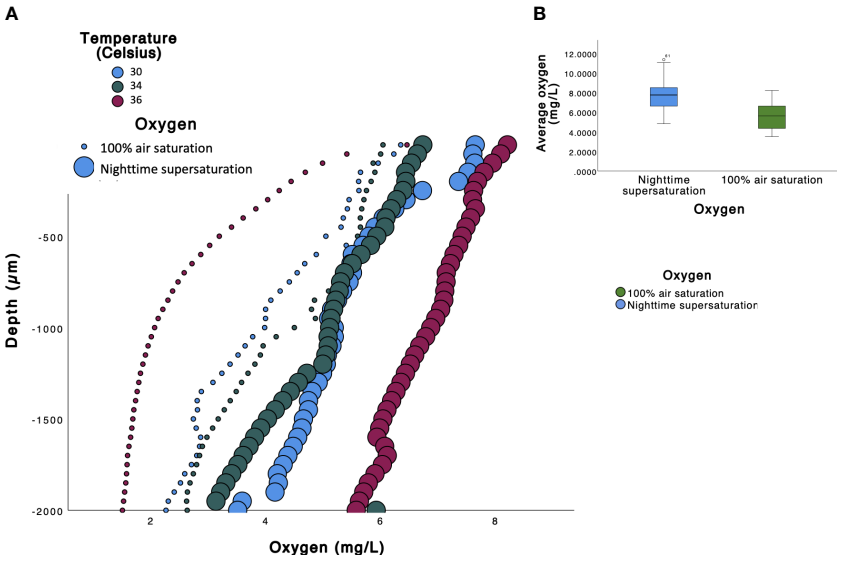

FIGURE 1
(A) Variability of O_2 levels (mg L^{-1}) within depth in the *Cassiopea andromeda* oral arms (µm) during nighttime under our experimental conditions. Each line represents the average of single profiles (n =3) within a one oral arm per replicate holobiont. **(B)** Boxplot representing the mean O_2 levels in the two treatments inside the oral arms ± standard error ($p < 0.001$, 1 SE). "NSS" (blue), and "100AS" (green). The black line in the boxes indicates the median ± standard error (1 SE).

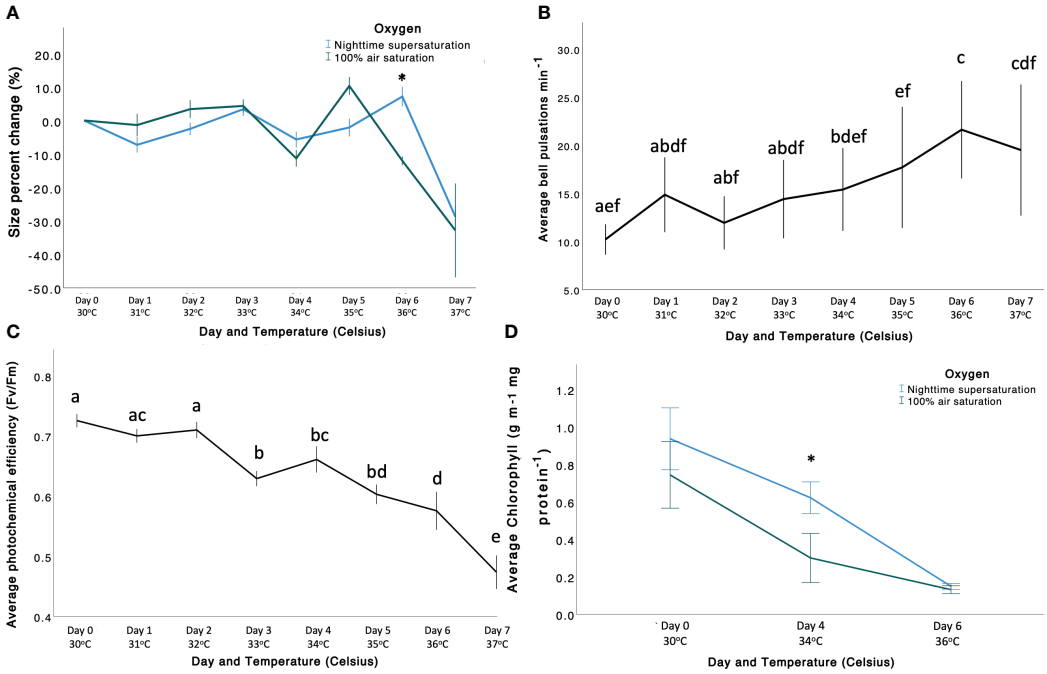

FIGURE 2
(A) Size percent change (PC, %) of *Cassiopea andromeda* in the two treatments ("NSS" in blue, and "100AS" in green). Size PC (%) is shown on the y-axis, whereas the x-axis shows the day and temperature (Celsius). **(B)** Average bell pulsation rate min^{-1} throughout the experiment shown according to significant factor (temperature). Average bell pulsations are shown on the y-axis, whereas the x-axis shows both temperature (Celsius) and day number. **(C)** Average photochemical efficiency (*Fv/Fm*) of *C. andromeda* throughout the experiment. Average photochemical efficiency is shown on the y-axis, whereas the x-axis shows both temperature (Celsius) and day number. **(D)** Average chlorophyll (μg mL^{-1} mg $protein^{-1}$) shown according to significant factor (temperature). Average chlorophyll is shown on the y-axis, whereas the x-axis shows both temperature (Celsius) and day number. In all the figures bars represent standard error (± 1 SE). Asterisk represents the significance of the difference between the two O_2 levels ($p < 0.005$).

Chlorophyll-*a* concentrations differed among the O_2 treatments, but the trend depended on the temperature, resulting in a significant Oxygen × Temperature interaction (Supplementary Table 7). Overall, the chlorophyll content decreased with increasing temperature, reaching a minimum at 36°C (Supplementary Table 9). Specifically, chlorophyll levels were similar at 30°C (0.833 ± 0.061 μg ml^{-1} mg $protein^{-1}$), but differed at 34°C (p-value = 0.002; Supplementary Table 8) in "NSS" (0.622 ± 0.042 μg ml^{-1} mg $protein^{-1}$) and in "100AS" (0.266 ± 0.062 μg ml^{-1} mg $protein^{-1}$). Thus, the loss in photosynthetic pigments (i.e. a proxy for bleaching) was mitigated by 42.73% at sublethal temperatures by "NSS". Then, at 36°C, they were similar again (0.140 ± 0.007 μg ml^{-1} mg $protein^{-1}$), reaching the minimum concentration before the end of the experiment, when all the holobionts died.

Notably, no effect of the O_2 treatments, temperature, or their interaction was observed for symbiont density (averaged 625.65 ± 55.59 × 10^4 cells ml^{-1}; Supplementary Table 7; Supplementary Figures 7, 8), glutathione-S-transferase (GST) activity (averaged 4.77 × 10^{-6} ± 3.74 × 10^{-7} μmol ug^{-1} protein min^{-1}; Supplementary Figure 10) and superoxide dismutase activity (averaged 21.69 ± 0.69 μmol $μg^{-1}$ protein min^{-1}; Supplementary Figure 11). We found that, independently from the treatment, all *C. andromeda* individuals primarily harboured Symbiodiniaceae of the genus *Symbiodinium*, corresponding to *Symbiodinium microadriaticum*, although a small proportion of clade C (genus Cladocopium; Hume et al., 2019) was found in one individual (similar results in Lampert et al., 2012; Supplementary Figure 12).

Diversity of bacterial communities

The three sample categories (i.e. holobionts, seawater and *Artemia*) hosted significantly different bacterial communities (manyglm; $Dev_{4,109}$ = 29,448; $p < 0.001$) with a clear separation between environmental samples and those used in the aquaria subjected to acclimated and incubation (Supplementary Figure 14). Notably, in the aquaria, a limited portion of OTUs was shared among feed, holobionts, and seawater (6%; Supplementary Figure 15). Such partition of the bacterial communities can be linked with the unicity of the three types of samples that impose different selective forces on the environmental microbiome. Therefore, to disentangle the fine-scale differences mediated by O_2 and temperature on *Cassiopea*'s bacterial community diversity, we excluded the seawater and *Artemia* samples in further analyses. Principal coordinates analysis (PCoA) highlighted the significant effect of the interaction among temperature and O_2 (manyglm: $Dev_{3,63}$ = 1272.579, $p < 0.001$). All the treatments (i.e. combinations of temperature and O_2 conditions) defined significantly different bacterial communities (Supplementary Table 12). This bacterial diversity increased with

10.3389/fmars.2024.1305674

the temperature decay in both "100AS" and "NSS", with differentiation of the microbiome increasing with warming (Supplementary Figure 16). When changes in O_2 treatments and temperature were considered, the holobionts bacterial communities had different dispersions (distance from centroid within a group); while during "NSS" the dispersion of bacterial communities significantly decreased with increasing temperature, the one in "100AS" was not affected (Figure 3B, ANCOVA $F_{1,67}$ = 5.64, p=0.02). This trend was consistently observed during the heating stress, determining a significantly higher dispersion in "100AS" than "NSS" (Figure 3C). At the same time, warming significantly increased richness (number of OTUs) under "NSS" ($F_{1,34}$ = 9.91, p = 0.0034, R^2 = 0.23, slope = 3.171; Supplementary Figures 18A, B).

The holobiont oral arms were dominated by bacterial members of *Bacteroidia* (32% of relative abundance), *Bacilli* (30.4%), *Alphaproteobacteria* (21.6%), *Oligoflexia* (10.4%), *Gammaproteobacteria* (3.3%), *Sericytochromatia* (1.4%), *Cyanobacteria* (0.4%) and *Verrucomicrobiae* (0.3%), along with a series of low abundant taxa (relative abundance, < 0.1%) that altogether account for less than 1% of the relative abundance (Figure 3D). At the compositional level, the effect of O_2 regimes between temperatures was further emphasized by the differential enrichment of specific bacterial taxa (Log_2fold-change > |2| and p < 0.05; Figure 3D). The "NSS" treatment enriched specific taxa, and they increased with the increase in temperature, passing from 9 taxa at 30°C and 34°C to 17 and 32 taxa at 36°C and 38°C, respectively (see blue branches in Figure 4). The "NSS" drove the enrichment of bacteria belonging to the *Bacterioidia* class (e.g., the *Flavobacteriaceae* family and the *Tenacibaculum* genus). However, the combination of supersaturation and heat-stress mediated the enrichment of different bacterial taxa positively correlated with temperature, including members of other groups within *Bacterioidia*, and of *Alphaproteobacteria*, *Gammaproteobacteria* and *Desulfobacteria* (Supplementary Figure 17). For instance, at 38°C, we observed an enrichment of *Vibrio* (*Gammaproteobacteria*), *Bradymonadales* (*Desulfobacteria*) and SM1A02 (*Phycisphaeraceae*), along with that of *Chitinophagales*, *Saprospiraceae*, *Nonlabens*, *Winogradskyella* and *Rhodobacteraceae* (*Pelagibaca*, *Paracoccus*, *Shimia* and *Ruegeria*) within *Bacterioidia*, and of *Parvularculaceae* (*Parvularcula*) and *Sphingomonadaceae* (*Erythrobacter*) within *Alphaproteobacteria* (Figure 4). Among these bacteria, common aquaculture parasites and pathogens were found, such as the *Vibrio* and *Tenacibaculum* (Avendaño-Herrera et al., 2004; Chatterjee and Haldar, 2012), along with potentially beneficial bacteria like the strictly aerobic photoheterotropher *Erythrobacter* (Hu et al., 2017).

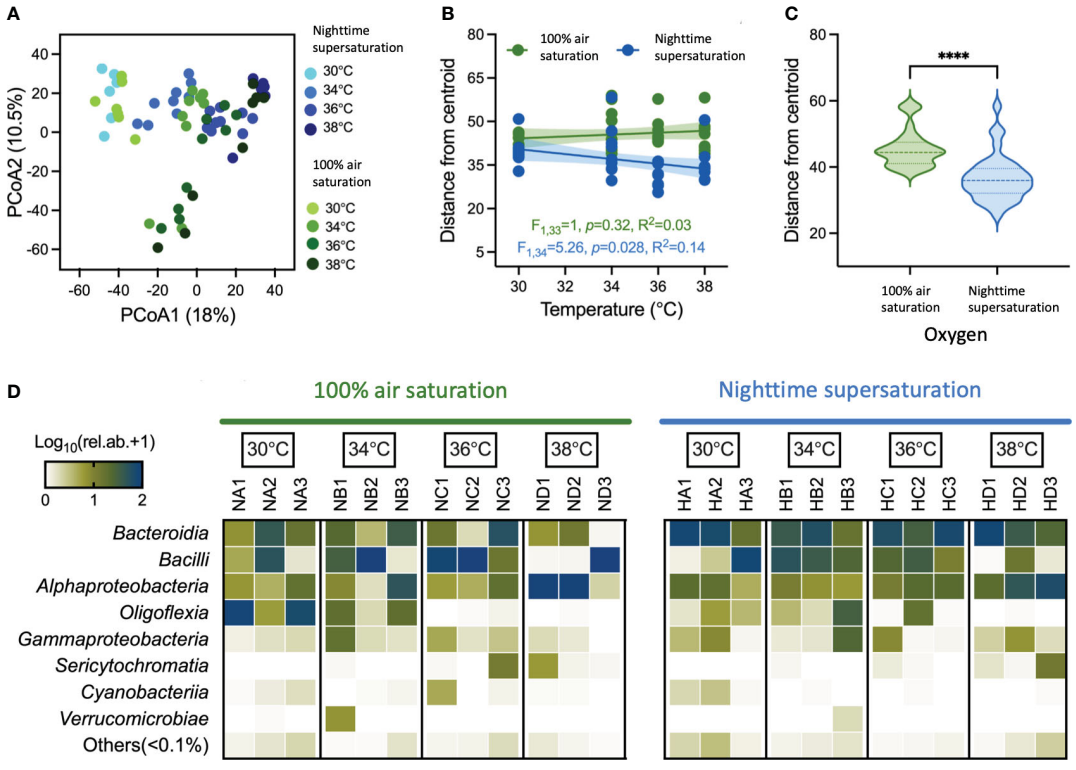

FIGURE 3
Patterns of bacterial diversity associated with *Cassiopea andromeda* holobionts oral arms. **(A)** Differences in community composition are shown in the principal coordinate analysis (PCoA) ordination space based on the Bray-Curtis similarity. Samples are grouped based on O_2 treatments ("100AS" on the green scale and "NSS" on the blue scale) and temperature (30°C, 34°C, 36°C and 38°C). **(B)** Temperature decay patterns of holobionts bacterial communities in "100AS" and "NSS" conditions show the relationships between differences in temperature and the distance from the centroid obtained from PERMDISP; the relationship is tested by linear regression (R^2) with a significance probability estimate (p-value). **(C)** Violin plots show the median and interquartile range of distance from the centroid. Stars indicate significant differences based on t-test comparisons (p < 0.0001). **(D)** Heat map shows the log-transformed relative abundance of the main bacterial classes associated with holobionts across different temperatures in "100AS" and "NSS" treatments; taxa belong to classes with relative abundance <0.1% are reported as 'Others'.

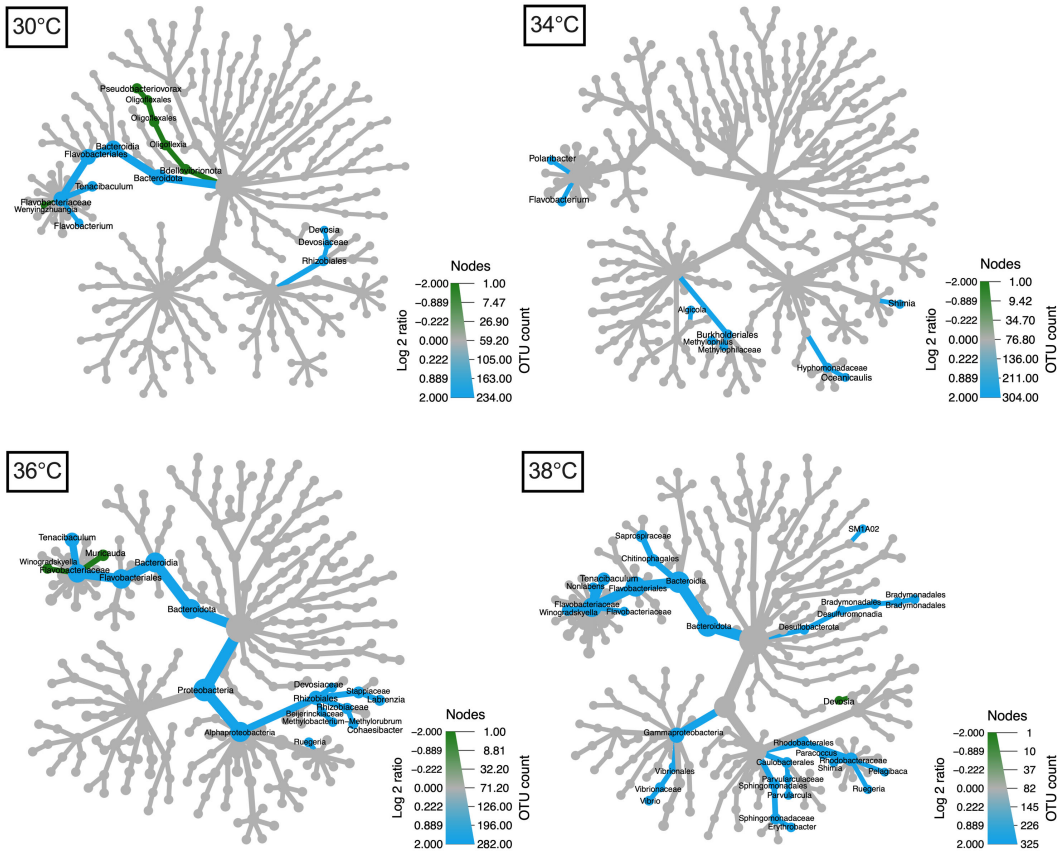

FIGURE 4
Differential abundance analyses highlight taxonomic differences between "100AS" and "NSS" assemblages across the bacterial tree at different temperatures. Taxonomic trees show over-represented bacterial taxa in the holobionts oral arms in "100AS" (green) and in "NSS" (blue). Each taxonomic tree includes one tested temperature (30°C – 38°C). The size of the nodes is directly correlated with the abundance of bacteria within each O_2 treatment.

The compositional differences driven by the synergistic effect of temperature and O_2 observed were also reflected in the differential predicted functional profiles of bacterial communities (CAP, p = 0.001), accompanied by an increased functional redundancy (Wemheuer et al., 2020) under "NSS" ($F_{1,34}$ = 9.91, p = 0.0034, R^2 = 0.23, slope = 3.171; Supplementary Figures 17C, D). An enrichment of N-cycle metabolisms was observed under "NSS" with increasing temperatures, as well as fermentation, cellulolytic and methylotrophic metabolisms, intracellular parasites and non-photosynthetic cyanobacteria (Supplementary Figure 19). On the contrary, photosynthetic metabolisms (Cyanobacteria-mediated, autotrophic, and heterotrophic) had an opposite trend with a reduction already at 34°C (Supplementary Figure 19).

Discussion

This study investigated the potential benefit of O_2 supersaturation (>140% air saturation; Giomi et al., 2019) in the Cnidaria-Symbiodiniaceae relationship in an acute thermal stress experiment. Our findings provide evidence that O_2 supersaturation adds resistance to the *Cassiopea andromeda* holobiont to moderate warming by mitigating size decrease, pigmentation loss, and by driving microbiome shifts. While the benefits of supersaturation are modest and observed only at moderate temperatures, we think this insight reveals a hidden advantage of this symbiosis.

Elevated temperatures alone impact the behavior (Banha, 2018; Klein et al., 2019; Béziat and Kunzmann, 2022) and physiology of marine cnidarians (Hoegh-Guldberg and Smith, 1989; Aljbour et al., 2017; Klein et al., 2019), potentially destabilizing the symbiosis with Symbiodiniaceae (LaJeunesse et al., 2018). Such thermal stress typically results in pigmentation loss due to decreased symbiont density (Yonge and Nicholls, 1931) and/or photosynthetic pigments (Hoegh-Guldberg and Smith, 1989), often accompanied by photochemical efficiency disruption (Warner et al., 1996). Warming-induced deoxygenation and increased O_2 demands (Vaquer-Sunyer and Duarte, 2011) further contribute to lowering the thermal thresholds of coral holobionts (Alderdice et al., 2022) and to the amplification of potential negative effects. However, in Cnidarian holobionts, supersaturation naturally occurs during the daytime when symbionts productivity dominates and coincides with peak temperatures. This increased O_2 availability was showed to mitigate the effects of thermal stress on non-symbiotic species (Pörtner et al., 2006; Giomi et al., 2019) by meeting the metabolic O_2 demand (Pörtner, 2012) and by enhancing the food/nutrient storage and usage (Stoner et al.,

2022) and might perform similarly in the Cnidarian holobiont. This was already confirmed in calcifying cnidarians, where increased O_2 availability enhanced calcification (Colombo-Pallotta et al., 2010). This explains the ~10.37% mitigation of size decrease under NSS, compared to holobionts under 100AS (-23.039% ± 0.687% vs. -33.418% ± 0.345%). Conversely, studies focusing solely on heat stress demonstrate >40% bell size reduction (Klein et al., 2019; Béziat and Kunzmann, 2022). While this mitigation occurs during moderate sublethal temperatures (36°C), it diminishes at the highest temperature. Within these conditions, chlorophyll-*a* loss was mitigated by 42.73% compared to 100AS. However, beyond a threshold (here, 34°C), excessive thermal stress overrides O_2 supply's chlorophyll-*a* preservation capacity. Oxygen supersaturation also fails to counteract photochemical efficiency decline under moderate thermal stress. These processes collectively precede the holobiont association breakdown (Warner et al., 1999). Nevertheless, our study shows that under moderate thermal stress, symbiont density remains stable irrespective of oxygen treatment, highlighting *Cassiopea*-Symbiodiniaceae relationship resilience (similar to Klein et al., 2019 where symbiont loss occurred above 37°C). Similarly, in other cnidarian holobionts (e.g., corals), photosynthesis ceases before symbiosis disruption (Warner et al., 1999), implying supersaturation's efficacy depends on sustained photosynthesis at elevated temperatures.

Exposure to elevated O_2 and high temperature can increase oxidative stress and Reactive Oxygen Species (ROS) production in cnidarians (Lesser, 2011; Roth, 2014; Aljbour et al., 2019). ROS can lead to cellular damage *via* a range of processes, such as lipid peroxidation, protein oxidation, and DNA degradation (Richier et al., 2005). However, damage occurs only when an imbalance between ROS production and antioxidant defenses is observed (Richier et al., 2005). Thus, in our experiment, variations in antioxidant enzymes, such as Superoxide Dismutase (SOD, the first line of defence against ROS; Hellou et al., 2012) and Glutathione-S-Transferase (GST, the second line of defence; Fridovich, 1995; Hayes and McLellan, 1999), were expected under our experimental conditions. However, no significant increase in antioxidant defenses due to either O_2 treatment or temperature was observed. The not significant responses of scavenging enzymes observed here might be explained by the increase in BPR under thermal stress, that likely reduces internal ROS concentration *via* ventilation (Welsh et al., 2009; Béziat and Kunzmann, 2022; Durieux et al., 2023), resulting in modest responses of scavenging enzymes. Alternatively, the minimal antioxidant responses observed may be attributed to the discrepancy in oxygen levels among replicates. While surrounding seawater exhibited oxygen concentrations above 9 mg L^{-1}, internal measurements within *Cassiopea* indicated lower levels, around 7.5 mg L^{-1}. Although this represents considerable oxygen supersaturation, as it is higher than 100% air saturation, in some individuals, ventilation was insufficient to achieve oxygen levels equal to those naturally observed internally (Arossa et al., 2021), especially at the deepest point investigated within the oral arms (below 600 µm, consistent with Arossa et al., 2021). The symbionts are indeed found in the upper part of the oral arms (Lyndby et al., 2020). This potentially influenced the observed outcomes and led to some degree of variability. Finally, other components of the holobiont (e.g., microbiome or other physiological pathways) may contribute to mitigating oxidative stress (e.g., Berkelmans and Van Oppen, 2006).

Given the multi-player nature of this symbiosis (i.e. the Bacteria-Cnidaria-Symbiodiniaceae relationship; Kwong et al., 2019), changes in environmental factors, such as temperature and O_2, are reflected in modifications of the Cnidaria-associated bacterial communities (e.g., Carabantes et al., 2022). In turn, shifts in the microbiome can shape the holobiont's tolerance to environmental stressors. For instance, heat-associated bacteria can confer protection mechanisms to their hosts (Hector et al., 2022) by enhancing the production of protective compounds against oxidative stress or heat-shock proteins (Berkelmans and Van Oppen, 2006). Notably, the bacterial microbiome can shape the holobiont's responses to environmental disturbance (Ainsworth et al., 2010; Hector et al., 2022). In our experiment, the interactive effect of O_2 and temperature affects the composition of the bacterial community associated with the *C. andromeda* holobionts, defining unique bacterial assemblages at taxonomic and predicted functional levels. Significant decrease of the dispersion of the bacterial community was observed at with the increase of temperatures associated with oxygen supersaturation suggesting that this treatment select a more consistent bacterial community (See Figure 3D; Hector et al., 2022). For example, in corals, the microbiome enhances the thermal tolerance of the polyps and in preventing bleaching events (Ziegler et al., 2017). This is corroborated by manipulative studies showing that coral survival under stressful events can be improved by enriching the microbiome with beneficial microorganisms (Santoro et al., 2021).

The limitation of the bacterial community dispersion driven by supersaturation can be considered an ecologically relevant contributor to the thermal tolerance of the holobiont. In our case, supersaturation significantly determined the enrichment (from 2 to 100-fold-change; Supplementary Table 1) of specific bacterial taxa at higher temperatures (36°C and 38°C), including the strict aerobic *Erythrobacter* sp., which can produce antioxidants (Jeong et al., 2022). Supersaturation also enriched other members of *Alphaproteobacteria* class, which accounts for many bacteria able to establish a symbiotic relationship with marine organisms (Dubilier et al., 2008). Although the functions of these bacterial taxa cannot be assessed, functionality prediction analysis revealed that following thermal stress, supersaturation increases the functional redundancy, possibly favouring the stability and resilience of the holobiont to disturbances (Biggs et al., 2020; Hector et al., 2022). After death (38°C), the growth of free-living aerobic heterotrophic bacteria (e.g., *Vibrio* and *Tenacibaculum*, typical of environmental deterioration, bleaching, and blooming events; Tinta et al., 2019) is favoured.

In fact, the presence of *Vibrio* can be justified by the nutrient-rich habitat provided by alive *Cassiopea* sp. specimens as well as by its decaying tissue, especially under higher temperature. *Vibrio* can be responsible for haemolysis, and cytotoxicity and they can outcompete other bacterial associates and become highly dominant (Kramar et al., 2019).

Moreover, the higher oxygen availability (NSS) favours the selection of less dispersed and richer aerobic bacterial member not enriched in condition of 100% oxygen saturation. Hence, further

investigations are essential to verify the role of the microbiome in our experimental conditions. This is imperative since additional physiological responses, not encompassed by our analyses, could potentially contribute to this observed phenomenon.

Overall, while no significant impact was observed on symbiont density, GST, and SOD activity across treatments, thermal stress led to a decline in chlorophyll content, photochemical efficiency, bell size, and an increase in bell pulsation rate. Oxygen supersaturation, particularly at moderate temperatures, mitigated chlorophyll and bell size reduction, indicating improved energy utilization and storage potential for the holobiont (Stoner et al., 2022). The microbiome may amplify these effects by enhancing oxidative stress defenses and overall holobiont resilience during moderate thermal stress (Hector et al., 2022), although further inquiry is needed. In these scenarios, the benefits of oxygen supersaturation disappeared once a certain threshold temperature is reached (e.g., 34 or 36°C, depending on the response), suggesting their efficacy within a specific temperature range. Notably, as many Cnidarians exist near their upper temperature limits (Klein et al., 2019), these benefits may not extend universally. In our experiment, mortality at 38°C remained consistent across oxygen treatments, highlighting that these responses to heat stress stem from intricate partner interactions (Hawkins et al., 2016; Klein et al., 2022), and may ultimately lead to holobiont's mortality. In this study, both experimental treatments were characterized by oxygen concentrations that exceeded oxygen values experienced by the holobiont during the nighttime under ambient temperature conditions (Arossa et al., 2021). Consequently, holobionts subjected to the treatment simulating "100AS" might have experienced a relative advantage during nighttime periods. Under typical hypoxic nighttime conditions, these organisms are indeed forced to navigate the challenges associated with reduced oxygen availability. This was taken into account for the discussion of the results.

Our study encountered specific limitations that shaped its execution and findings. First, the inclusion of a temperature control group, while ideal, was not feasible due to the experiment's sacrificial nature and the limited availability of holobionts. This limitation, however, allowed us to focus on enhancing the statistical power for more robust inter-treatment comparisons. Second, our experimental design did not incorporate a real control in the natural environment, presenting a potential gap in simulating the exact environmental contexts our findings might apply to. Third, we faced technical limitations with our gas delivery system, which prevented us from achieving the target oxygen levels for the supersaturation treatment. Each of these constraints played a role in shaping the scope and interpretation of our results.

In conclusion, during thermal stress, *C. andromeda* holobionts gain from supersaturation through (1) stabilizing bell size, (2) mitigating loss of photosynthetic pigments, (3) the selection of a more consistent bacterial community, and (4) enhancing bacterial community redundancy for heightened holobiont resilience. Thus, the increased O_2 supply from external primary producers isn't the sole factor driving thermal resilience; *Cassiopea's* endosymbionts likely contribute significantly. These findings align with Banha et al. (2020) that *C. andromeda* could thrive in future climate change scenarios of elevated seawater temperatures, expanding its range (Aljbour et al., 2019) where supersaturation environmentally prevails or thanks to the photosynthetic activity of endosymbionts. Nonetheless, investigating whether these outcomes apply to other cnidarian holobiont associations remains imperative. While this research highlights the benefits of Symbiodiniaceae driven O_2 supersaturation for cnidarians, expanding ocean deoxygenation, particularly in warm waters such as the Red Sea, underscores the urgent need to address eutrophication and global CO_2 emissions, and restore potential sources of O_2 (e.g., seagrass meadows, mangroves, etc.). These factors are significant anthropogenic contributors to the formation of oxygen-depleted zones.

Data availability statement

Raw sequence data of microbiome analyses have been deposited in the Sequence Read Archives with NCBI BioProject accession no. PRJNA964583. ITS2 sequencing data have been deposited in the Sequence Read Archives with NCBI BioProject accession no. PRJNA966908 R Script code for microbiome analyses is available at: https://github.com/MarcoFusi1980/Cassiopea. Data of all the other biological responses are submitted as supplementary file named "Supplementary Data 1".

Author contributions

SA: Conceptualization, Data curation, Formal analysis, Investigation, Methodology, Visualization, Writing – original draft, Writing – review & editing. SK: Conceptualization, Investigation, Methodology, Supervision, Validation, Writing – review & editing. EG: Writing – review & editing, Validation, Methodology, Investigation, Data curation, Conceptualization. AS: Writing – review & editing, Investigation. AP: Writing – review & editing, Investigation. JA: Writing – review & editing, Investigation. TA: Investigation, Writing – review & editing. XY: Investigation, Writing – review & editing. S-HH: Writing – review & editing, Investigation, Methodology. OM: Methodology, Validation, Visualization, Writing – review & editing, Investigation. RM: Formal analysis, Investigation, Methodology, Supervision, Validation, Visualization, Writing – review & editing, Writing – original draft. MF: Writing – original draft, Writing – review & editing, Visualization, Validation, Software, Methodology, Investigation, Formal analysis, Data curation. MA: Writing – review & editing, Resources, Funding acquisition, Conceptualization. DD: Writing – review & editing, Supervision, Resources, Funding acquisition. CD: Writing – review & editing, Validation, Supervision, Resources, Funding acquisition, Conceptualization.

Funding

The author(s) declare financial support was received for the research, authorship, and/or publication of this article. Financial support for this research was provided by the King Abdullah

University of Science and Technology and the Tarek Ahmed Juffali Research Chair on Red Sea Ecology, including the baseline research funds of CD, MA, and the Competitive Research Grant (CRG-7-3739) assigned to DD, "The role of the bacterial symbiome at the gill - water (air) interface in the evolution towards terrestrialization (Microlanding)", 1 April 2019 to 31 March 2022.

Acknowledgments

We thank the KAUST Coastal and Marine Resources Coral Labs (CMOR) team for their support and assistance.

Conflict of interest

The authors declare that the research was conducted in the absence of any commercial or financial relationships that could be construed as a potential conflict of interest.

The author(s) declared that they were an editorial board member of Frontiers, at the time of submission. This had no impact on the peer review process and the final decision

Publisher's note

Supplementary material

The Supplementary Material for this article can be found online at: https://www.frontiersin.org/articles/10.3389/fmars.2024.1305674/full#supplementary-material

References

Ainsworth, T. D., Thurber, R. V., and Gates, R. D. (2010). The future of coral reefs: a microbial perspective. *Trends Ecol. Evol.* 25, 233–240. doi: 10.1016/j.tree.2009.11.001

Alderdice, R., Perna, G., Cárdenas, A., Hume, B. C., Wolf, M., Kühl, M., et al. (2022). Deoxygenation lowers the thermal threshold of coral bleaching. *Sci. Rep.* 12, 18273. doi: 10.1038/s41598–022-22604–3

Aljbour, S. M., Zimmer, M., Al-Horani, F. A., and Kunzmann, A. (2019). Metabolic and oxidative stress responses of the jellyfish *Cassiopea* sp. to changes in seawater temperature. *J. Sea Res.* 145, 1–7. doi: 10.1016/j.seares.2018.12.002

Aljbour, S. M., Zimmer, M., and Kunzmann, A. (2017). Cellular respiration, oxygen consumption, and trade-offs of the jellyfish *Cassiopea* sp. in response to temperature change. *J. Sea Res.* 128, 92–97. doi: 10.1016/j.seares.2017.08.006

Anderson, M. J., and Walsh, D. C. (2013). PERMANOVA, ANOSIM, and the Mantel test in the face of heterogeneous dispersions: what null hypothesis are you testing? *Ecol. Monogr.* 83, 557–574. doi: 10.1890/12-2010.1

Arossa, S., Barozzi, A., Callegari, M., Klein, S. G., Parry, A. J., Hung, S. H., et al. (2021). The internal microenvironment of the symbiotic jellyfish *Cassiopea* sp. From the red sea. *Front. Mar. Sci.* 8. doi: 10.3389/fmars.2021.705915

Avendaño-Herrera, R., Magariños, B., López-Romalde, S., Romalde, J. L., and Toranzo, A. E. (2004). Phenotypic characterization and description of two major o-serotypes in tenacibaculum maritimum strains from marine fishes. *Dis. Aquat. Organisms* 58 (1), 1–8.

Banha, T. N. S. (2018). *Experimental effects of multiple thermal stress events on chlorophyll-a content and size of* Cassiopea andromeda *and the role of heterotrophic feeding and* Symbiodinium *concentration*. Dissertação (Mestrado em Oceanografia Biológica). São Paulo: Instituto Oceanográfico, University of São Paulo. doi: 10.11606/D.21.2019.tde-11022019–143521

Banha, T. N., Mies, M., Güth, A. Z., Pomory, C. M., and Sumida, P. Y. (2020). Juvenile *Cassiopea andromeda* medusae are resistant to multiple thermal stress events. *Mar. Biol.* 167, 1–13. doi: 10.1007/s00227-020-03792-w

Berkelmans, R., and Van Oppen, M. J. (2006). The role of zooxanthellae in the thermal tolerance of corals: a 'nugget of hope' for coral reefs in an era of climate change. *Proc. R. Soc B* 273, 2305–2312. doi: 10.1098/rspb.2006.3567

Béziat, P., and Kunzmann, A. (2022). Under pressure: *Cassiopea andromeda* jellyfish exposed to increasing water temperature or lead, cadmium and anthropogenic gadolinium contamination. *Mar. Biol. Res.* 18 (1-2), 48–63. doi: 10.1080/17451000.2022.2066132

Biggs, C. R., Yeager, L. A., Bolser, D. G., Bonsell, C., Dichiera, A. M., Hou, Z., et al. (2020). Does functional redundancy affect ecological stability and resilience? A review and meta-analysis. *Ecosphere* 11, e03184. doi: 10.1002/ecs2.3184

Bolyen, E., Rideout, J. R., Dillon, M. R., Bokulich, N. A., Abnet, C. C., Al-Ghalith, G. A., et al. (2019). Reproducible, interactive, scalable and extensible microbiome data science using QIIME 2. *Nat. Biotechnol.* 37, 852–857. doi: 10.1038/s41587-019-0209-9

Brune, A., Emerson, D., and Breznak, J. A. (1995). The termite gut microflora as an oxygen sink: microelectrode determination of oxygen and pH gradients in guts of lower and higher termites. *Appl. Environ. Microbiol.* 61, 2681–2687. doi: 10.1128/aem.61.7.2681-2687.1995

Carabantes, N., Cerqueda-García, D., García-Maldonado, J. Q., and Thomé, P. E. (2022). Changes in the bacterial community associated with experimental symbiont loss in the mucus layer of *Cassiopea xamachana* jellyfish. *Front. Mar. Sci.* 9, 879184. doi: 10.3389/fmars.2022.879184

Chaidez, V., Dreano, D., Agusti, S., Duarte, C. M., and Hoteit, I. (2017). Decadal trends in Red Sea maximum surface temperature. *Sci. Rep.* 7, 1–8. doi: 10.1038/s41598-017-08146-z

Chatterjee, S., and Haldar, S. (2012). Vibrio related diseases in aquaculture and development of rapid and accurate identification methods. *J. Mar. Sci. Res. Dev.* S1–002, 1–7. doi: 10.4172/2155–9910.S1–002

Claret, M., Galbraith, E. D., Palter, J. B., Bianchi, D., Fennel, K., Gilbert, D., et al. (2018). Rapid coastal deoxygenation due to ocean circulation shift in the northwest atlantic. *Nat. Climate Change* 8 (10), 868–872. doi: 10.1038/s41558-018-0263-1

Colombo-Pallotta, M. F., Rodríguez-Román, A., and Iglesias-Prieto, R. (2010). Calcification in bleached and unbleached Montastraea faveolata: evaluating the role of oxygen and glycerol. *Coral Reefs* 29, 899–907. doi: 10.1007/s00338-010-0638-x

Deutsch, C., Brix, H., Ito, T., Frenzel, H., and Thompson, L. (2011). Climate-forced variability of ocean hypoxia. *Science* 333, 336–339. doi: 10.1126/science.1202422

Diaz, J. M., Hansel, C. M., Apprill, A., Brighi, C., Zhang, T., Weber, L., et al. (2016). Species-specific control of external superoxide levels by the coral holobiont during a natural bleaching event. *Nat. Commun.* 7, 13801. doi: 10.1038/ncomms13801

Dubilier, N., Bergin, C., and Lott, C. (2008). Symbiotic diversity in marine animals: the art of harnessing chemosynthesis. *Nat. Rev. Microbiol.* 6, 725–740. doi: 10.1038/nrmicro1992

Dungan, A. M., Maire, J., Perez-Gonzalez, A., Blackall, L. L., and van Oppen, M. J. (2022). Lack of evidence for the oxidative stress theory of bleaching in the sea anemone, exaiptasia diaphana, under elevated temperature. *Coral Reefs* 41 (4), 1161–1172. doi: 10.1007/s00338-022-02251-w

Durieux, D. M., Scrogham, G. D., Fender, C., Lewis, D. B., Deban, S. M., and Gemmell, B. J. (2023). Benthic jellyfish act as suction pumps to facilitate release of interstitial porewater. *Sci. Rep.* 13, 3770. doi: 10.1038/s41598-023-30101-4

Fitzpatrick, C. R., Lu-Irving, P., Copeland, J., Guttman, D. S., Wang, P. W., Baltrus, D. A., et al. (2018). Chloroplast sequence variation and the efficacy of peptide nucleic acids for blocking host amplification in plant microbiome studies. *Microbiome* 6, 144. doi: 10.1186/s40168-018-0534-0

Freeman, C. J., Stoner, E. W., Easson, C. G., Matterson, K. O., and Baker, D. M. (2016). Symbiont carbon and nitrogen assimilation in the *Cassiopea Symbiodinium* mutualism. *Mar. Ecol. Prog. Ser.* 544, 281–286. doi: 10.3354/meps11605

Fridovich, I. (1995). Superoxide radical and superoxide dismutases. *Annu. Rev. Biochem.* 64, 97–112. doi: 10.1146/annurev.bi.64.070195.000525

Furla, P., Richier, S., and Allemand, D. (2011). Physiological adaptation to symbiosis in cnidarians. *Coral reefs: an ecosystem transition*, 187–195.

Giomi, F., Barausse, A., Duarte, C. M., Booth, J., Agusti, S., Saderne, V., et al. (2019). Superoxygenation protects coastal marine fauna from ocean warming. *Sci. Adv.* 5, eaax1814. doi: 10.1126/sciadv.aax1814

Giomi, F., Barausse, A., Steckbauer, A., Daffonchio, D., Duarte, C. M., and Fusi, M. (2023). Oxygen dynamics in marine productive ecosystems at ecologically relevant scales. *Nat. Geosci.* 16 (7), 560–6. doi: 10.1038/s41561-023-01217-z

Halliwell, B., and Gutteridge, J. M. C. (1999). *Free radicals in biology and medicine. 3rd edn* (New York: Oxford University Press).

Hawkins, T., Hagemeyer, J., and Warner, M. (2016). Temperature moderates the infectiousness of two conspecific *Symbiodinium* strains isolated from the same host population. *Environ. Microbiol.* 18, 5204–5217. doi: 10.1111/1462-2920.13535

Hayes, J. D., and McLellan, L. I. (1999). Glutathione and glutathione-dependent enzymes represent a co-ordinately regulated defence against oxidative stress. *Free Radic. Res.* 31, 273–300. doi: 10.1080/10715769900300851

Hector, T. E., Hoang, K. L., Li, J., and King, K. C. (2022). Symbiosis and host responses to heating. *Trends Ecol. Evol.* 37 (7), 611–624. doi: 10.1016/j.tree.2022.03.011

Hellou, J., Ross, N. W., and Moon, T. W. (2012). Glutathione, glutathione S-transferase, and glutathione conjugates, complementary markers of oxidative stress in aquatic biota. *Environ. Sci. pollut. Res.* 19, 2007–2023. doi: 10.1007/s11356-012-0909-x

Herrera, M., Klein, S. G., Schmidt-Roach, S., Campana, S., Cziesielski, M. J., Chen, J. E., et al. (2020). Unfamiliar partnerships limit cnidarian holobiont acclimation to warming. *Global Change Biol.* 26, 5539–5553. doi: 10.1111/gcb.15263

Hoegh-Guldberg, O., and Smith, G. J. (1989). The effects of sudden changes in light, temperature and salinity on the population density and export of zooxanthellae from the reef corals *Seriatopora hystrix* and *Stylophora pistillata*. *J. Exp. Mar. Biol. Ecol.* 129, 279–303. doi: 10.1016/0022-0981(89)90109-3

Hu, X., Cao, Y., Wen, G., Zhang, X., Xu, Y., Xu, W., et al. (2017). Effect of combined use of Bacillus and molasses on microbial communities in shrimp cultural enclosure systems. *Aquacult. Res.* 48, 2691–2705. doi: 10.1111/are.2017.48.issue-6

Hughes, D. J., Alderdice, R., Cooney, C., Kühl, M., Pernice, M., Voolstra, C. R., et al. (2020). Coral reef survival under accelerating ocean deoxygenation. *Nat. Clim. Chang*, 296–307. doi: 10.1038/s41558-020-0737-9

Hume, B. C., Smith, E. G., Ziegler, M., Warrington, H. J., Burt, J. A., LaJeunesse, T. C., et al. (2019). SymPortal: A novel analytical framework and platform for coral algal symbiont next-generation sequencing ITS2 profiling. *Mol. Ecol. Resour* 19, 1063–1080. doi: 10.1111/1755-0998.13004

Jeong, S. W., Yang, J. E., and Choi, Y. J. (2022). Isolation and characterization of a yellow xanthophyll pigment-producing marine bacterium, Erythrobacter sp. SDW2 strain, in coastal seawater. *Mar. Drugs* 20, 73. doi: 10.3390/md2001007342

Klein, S. G., Geraldi, N. R., Anton, A., Schmidt-Roach, S., Ziegler, M., Cziesielski, M. J., Martin, C., et al (2022). Projecting coral responses to intensifying marine heatwaves under ocean acidification. *Global Change Biol.* 28 (5), 1753–1765. doi: 10.1111/gcb.15818

Klein, S. G., Pitt, K. A., Lucas, C. H., Hung, S. H., Schmidt-Roach, S., Aranda, M., et al. (2019). Night-time temperature reprieves enhance the thermal tolerance of a symbiotic cnidarian. *Front. Mar. Sci.* 6, 460582. doi: 10.3389/fmars.2019.00453

Klein, S. G., Steckbauer, A., and Duarte, C. M. (2020). Defining CO_2 and O_2 syndromes of marine biomes in the Anthropocene. *Glob. Change Biol.* 26, 355–363. doi: 10.1111/gcb.14879

Klein, S. G., Pitt, K. A., Nitschke, M. R., Goyen, S., Welsh, D. T., Suggett, D. J., et al. (2017). Symbiodinium mitigate the combined effects of hypoxia and acidification on a noncalcifying cnidarian. *Global Change Biol.* 23 (9), 3690–3703. doi: 10.1111/gcb.13718

Kramar, K. M., Tinta, T., Lučić, D., Malej, A., and Turk, V. (2019). Bacteria associated with moon jellyfish during bloom and post-bloom periods in the Gulf of Trieste (northern Adriatic). *PloS One* 14, e0198056. doi: 10.1371/journal.pone.0198056

Kühl, M., Cohen, Y., Dalsgaard, T., Jørgensen, B. B., and Revsbech, N. P. (1995). Microenvironment and photosynthesis of zooxanthellae in scleractinian corals studied with microsensors for O_2, pH and light. *Mar. Ecol. Prog. Ser.* 117, 159–172. doi: 10.3354/meps117159

Kwong, W. K., Del Campo, J., Mathur, V., Vermeij, M. J., and Keeling, P. J. (2019). A widespread coral-infecting apicomplexan with chlorophyll biosynthesis genes. *Nature* 568, 103–107. doi: 10.1038/s41586-019-1072-z

LaJeunesse, T. C., Parkinson, J. E., Gabrielson, P. W., Jeong, H. J., Reimer, J. D., Voolstra, C. R., et al. (2018). Systematic revision of Symbiodiniaceae highlights the antiquity and diversity of coral endosymbionts. *Curr. Biol.* 28, 2570–2580.e66. doi: 10.1016/j.cub.2018.07.008

Lampert, K. P., Bürger, P., Striewski, S., and Tollrian, R. (2012). Lack of association between color morphs of the Jellyfish Cassiopea andromeda and zooxanthella clade. *Mar. Ecol.* 33, 364–369. doi: 10.1111/j.1439-0485.2011.00488.x

Lesser, M. P. (2011). Coral bleaching: causes and mechanisms. *Coral reefs: an ecosystem transition*, 405–419.

Louca, S., Jacques, S. M., Pires, A. P., Leal, J. S., Srivastava, D. S., Parfrey, L. W., et al. (2016). High taxonomic variability despite stable functional structure across microbial communities. *Nat. Ecol. Evol.* 1 (1), 15. doi: 10.1038/s41559-016-0015

Lyndby, N. H., Rädecker, N., Bessette, S., Søgaard Jensen, L. H., Escrig, S., Trampe, E., et al. (2020). Amoebocytes facilitate efficient carbon and nitrogen assimilation in the Cassiopea-Symbiodiniaceae symbiosis. *Proc. R. Soc B* 287, 20202393. doi: 10.1098/rspb.2020.2393

McArley, T. J., Hickey, A. J., and Herbert, N. A. (2020). Acute high temperature exposure impairs hypoxia tolerance in an intertidal fish. *PloS One* 15 (4), e0231091. doi: 10.1371/journal.pone.0231091

Michoud, G., Ngugi, D. K., Barozzi, A., Merlino, G., Calleja, M. L., Delgado-Huertas, A., et al. (2021). Fine-scale metabolic discontinuity in a stratified prokaryote microbiome of a Red Sea deep halocline. *ISME J.* 15, 2351–2365. doi: 10.1038/s41396-021-00931-z

Nielsen, D. A., Petrou, K., and Gates, R. D. (2018). Coral bleaching from a single cell perspective. *ISME J.* 12, 1558–1567. doi: 10.1038/s41396-018-0080-6

Ohde, S., and van Woesik, R. (1999). Carbon dioxide flux and metabolic processes of a coral reef, Okinawa. *Bull. Mar. Sci.* 65, 559–576.

Pezner, A. K., Courtney, T. A., Barkley, H. C., Chou, W. C., Chu, H. C., Clements, S. M., et al. (2023). Increasing hypoxia on global coral reefs under ocean warming. *Nat. Clim. Change* 13 (4), 403–9. doi: 10.1038/s41558-023-01619-2

Pörtner, H. O., and Farrell, A. P. (2008). Physiology and climate change. *Science* 322, 690–692. doi: 10.1126/science.1163156

Pörtner, H. O., Peck, L. S., and Hirse, T. (2006). Hyperoxia alleviates thermal stress in the Antarctic bivalve, Laternula elliptica: evidence for oxygen limited thermal tolerance. *Polar Biol.* 29, 688–693. doi: 10.1007/s00300-005-0106-1

Pörtner, H. O. (2012). Integrating climate-related stressor effects on marine organisms: unifying principles linking molecule to ecosystem-level changes. *Mar. Ecol. Prog. Ser.* 470, 273–290. doi: 10.3354/meps10123

Richier, S., Furla, P., Plantivaux, A., Merle, P. L., and Allemand, D. (2005). Symbiosis-induced adaptation to oxidative stress. *J. Exp. Biol.* 208, 277–285. doi: 10.1242/jeb.01368

Richier, S., Merle, P. L., Furla, P., Pigozzi, D., Sola, F., and Allemand, D. (2003). Characterization of superoxide dismutases in anoxia- and hyperoxia-tolerant symbiotic cnidarians. *Biochim. Biophys. Acta* 1621, 84–91. doi: 10.1016/S0304-4165(03)00049-7

Robbins, S. J., Song, W., Engelberts, J. P., Glasl, B., Slaby, B. M., Boyd, J., et al. (2021). A genomic view of the microbiome of coral reef demosponges. *ISME J.* 15, 1641–1654. doi: 10.1038/s41396-020-00876-9

Roik, A., Röthig, T., Roder, C., Ziegler, M., Kremb, S. G., and Voolstra, C. R. (2016). Year-long monitoring of physico-chemical and biological variables provide a comparative baseline of coral reef functioning in the central Red Sea. *PloS One* 11, e0163939. doi: 10.1371/journal.pone.0163939

Roth, M. S. (2014). The engine of the reef: photobiology of the coral–algal symbiosis. *Front. Microbiol.* 5, 422. doi: 10.3389/fmicb.2014.00422

Saderne, V., Baldry, K., Anton, A., Agusti, S., and Duarte, C. M. (2019). Characterization of the CO_2 system in a coral reef, a seagrass meadow, and a mangrove forest in the central Red Sea. *J. Geophys. Res. Oceans* 124, 7513–7528. doi: 10.1029/2019JC015266

Safaie, A., Silbiger, N. J., McClanahan, T. R., Pawlak, G., Barshis, D. J., Hench, J. L., et al. (2018). High frequency temperature variability reduces the risk of coral bleaching. *Nat. Commun.* 9, 1671. doi: 10.1038/s41467-018-04074-2

Santoro, E. P., Borges, R. M., Espinoza, J. L., Freire, M., Messias, C. S., Villela, H. D., et al. (2021). Coral microbiome manipulation elicits metabolic and genetic restructuring to mitigate heat stress and evade mortality. *Sci. Adv.* 7, eabg3088. doi: 10.1126/sciadv.abg3088

Schuett, C., and Doepke, H. (2010). Endobiotic bacteria and their pathogenic potential in cnidarian tentacles. *Helgol. Mar. Res.* 64, 205–212. doi: 10.1007/s10152-009-0179-2

Stoner, E. W., Archer, S. K., and Layman, C. A. (2022). Increased nutrient availability correlates with increased growth of the benthic jellyfish *Cassiopea* spp. *Food Webs* 31, e00231. doi: 10.1016/j.fooweb.2022.e00231

Stramma, L., Johnson, G. C., Sprintall, J., and Mohrholz, V. (2008). Expanding oxygen-minimum zones in the tropical oceans. *Science* 320, 655–658. doi: 10.1126/science.1153847

Stramma, L., and Schmidtko, S. (2021). Spatial and temporal variability of oceanic oxygen changes and underlying trends. *Atmos. Ocean* 59, 122–132. doi: 10.1080/07055900.2021.1905601

Tinta, T., Kogovšek, T., Klun, K., Malej, A., Herndl, G. J., and Turk, V. (2019). Jellyfish-associated microbiome in the marine environment: exploring its biotechnological potential. *Mar. Drugs* 17, 94. doi: 10.3390/md17020094

Trowbridge, C. D., Davenport, J., Cottrell, D. M., Harman, L., Plowman, C. Q., Little, C., et al. (2017). Extreme oxygen dynamics in shallow water of a fully marine Irish sea lough. *Reg. Stud. Mar. Sci.* 11, 9–16. doi: 10.1016/j.rsma.2017.01.008

Vaquer-Sunyer, R., and Duarte, C. M. (2011). Temperature effects on oxygen thresholds for hypoxia in marine benthic organisms. *Glob. Change Biol.* 17, 1788–1797. doi: 10.1111/j.1365-2486.2010.02343.x

Verde, E. A., and McCloskey, L. R. (1998). Production, respiration, and photophysiology of the mangrove jellyfish *Cassiopea xamachana* symbiotic with zooxanthellae: effect of jellyfish size and season. *Mar. Ecol. Prog. Ser.* 168, 147–162. doi: 10.3354/meps168147

Voolstra, C. R., Buitrago-López, C., Perna, G., Cárdenas, A., Hume, B. C., Rädecker, N., et al. (2020). Standardized short-term acute heat stress assays resolve historical

differences in coral thermotolerance across microhabitat reef sites. *Glob. Change Biol.* 26, 4328–4343. doi: 10.1111/gcb.15148

Warner, M. E., Fitt, W. K., and Schmidt, G. W. (1996). The effects of elevated temperature on the photosynthetic efficiency of zooxanthellae in hospite from four different species of reef coral: a novel approach. *Plant Cell Environ.* 19, 291–299. doi: 10.1111/j.1365-3040.1996.tb00251.x

Warner, M. E., Fitt, W. K., and Schmidt, G. W. (1999). Damage to photosystem II in symbiotic dinoflagellates: a determinant of coral bleaching. *Proc. Natl. Acad. Sci. U.S.A.* 96, 8007–8012. doi: 10.1073/pnas.96.14.8007

Warner, M. E., and Suggett, D. J. (2016). "The photobiology of symbiodinium spp.: linking physiological diversity to the implications of stress and resilience," in *The Cnidaria, Past, Present and Future*, Goffredo, S., and Dubinsky, Z. (Cham: Springer). doi: 10.1007/978-3-319-31305-4_30

Welsh, D. T., Dunn, R. J., and Meziane, T. (2009). Oxygen and nutrient dynamics of the upside-down jellyfish (*Cassiopea* sp.) and its influence on benthic nutrient exchanges and primary production. *Hydrobiologia* 635, 351–362. doi: 10.1007/s10750-009-9928-0

Wemheuer, F., Taylor, J. A., Daniel, R., Johnston, E., Meinicke, P., Thomas, T., et al. (2020). Tax4Fun2: prediction of habitat-specific functional profiles and functional redundancy based on 16S rRNA gene sequences. *Environ. Microbiome* 15, 1–12. doi: 10.1186/s40793-020-00358-7

Yonge, C. M., and Nicholls, A. G. (1931). Studies on the physiology of corals. IV. The structure, distribution, and physiology of the zooxanthellae. *Sci. Rep. Great Barrier Reef Exped* 1928–29, 135–176.

Yu, L., Fennel, K., Laurent, A., Murrell, M., and Lehrter, J. (2015). Numerical analysis of the primary processes controlling oxygen dynamics on the Louisiana shelf. *Biogeosciences* 12, 2063–2076. doi: 10.5194/bg-12-2063-2015

Ziegler, M., Seneca, F. O., Yum, L. K., Palumbi, S. R., and Voolstra, C. R. (2017). Bacterial community dynamics are linked to patterns of coral heat tolerance. *Nat. Commun.* 8 (1), 14213.